PROCEEDINGS OF

SOLAR '95

THE 1995
AMERICAN SOLAR ENERGY SOCIETY
ANNUAL CONFERENCE

Minneapolis, Minnesota
July 15-20, 1995

Editors:
R. Campbell-Howe
B. Wilkins-Crowder

American Solar Energy Society
2400 Central Avenue, Suite G-1
Boulder, CO 80301

Printed on recycled paper

ANALYSIS OF A LOAD-SIDE HEAT EXCHANGER FOR A SOLAR DOMESTIC HOT WATER HEATING SYSTEM

Toni R. Smith
Patrick J. Burns
Douglas C. Hittle
Colorado State University
Mechanical Engineering Department
Solar Energy Applications Lab, SH II
Fort Collins, CO 80523

ABSTRACT

The Colorado State University Solar Energy Applications Laboratory is currently testing several solar domestic hot water systems. The experimental systems are fully instrumented to yield all data appropriate for in-depth analyses of performance. One of these systems is an unpressurized drainback system with a load-side heat exchanger. An analysis of the performance of this heat exchanger is the focus of this paper. Analytical calculations for the effectiveness and convective heat transfer coefficients from correlations are compared against the experimental data. The convective correlations yield heat transfer coefficients that underpredict the measured by as little as 17% and as much as 72%. TRNSYS simulations were performed using the average effectiveness; the results compare favorably with experimental results, indicating that a constant effectiveness is an adequate model for the system.

1. INTRODUCTION

Load-side heat exchangers are used in solar domestic hot water heating systems for several reasons. One such reason is to allow the use of an unpressurized storage tank; thus, a drainback system (to avoid freezing of the lines to and from the collector) could be used. Also, if the system is unpressurized, then the collectors can be designed for lower pressures. The use of a load-side heat exchanger eliminates the need for a pump on the load delivery side. The system tested is shown in Figure 1. To transfer the heat from the solar storage tank to the load water, mains supply, shown as point A, travels to point B via a dep-tube, and then is circulated through the coil that is submerged in the solar storage tank. The water enters the auxiliary tank at point C. This arrangement may also promote stratification, depending on the location of the coil, which can increase collector performance [Farrington and Bingham, 1987]. This type of heat exchanger operates only when a draw is occurring and is a "one-pass" system. In support of the Solar Ratings and Certification Corporation's (SRCC) ongoing work, validation of the model of the load-side heat exchanger is important.

2. SYSTEM DESCRIPTION AND INSTRUMENTATION

A comprehensive system instrumentation plan has been designed to effect system measurements of temperatures, electrical power input, flow rate, and differential pressure across the pumps. In addition, an outdoor ambient weather station has been designed and installed specifically for these tests. Measurements from the ambient weather station constitute inputs while system measurements constitute system states and outputs. A detailed test of the systems under actual operating conditions is the intent of these experiments. Outdoor and system measurements are made as indicated in Figure 1. Measurements are taken every 8 seconds. Three hot water draws are accomplished each day at 8 a.m., noon, and 4 p.m., as per ASHRAE standard 95-85. The test data were acquired for the time period of July 24 - 28, 1994. All temperature measurements are made with high-grade type T (Copper/Constantin) thermocouples. It is essential that extremely accurate temperature measurements be made, as the temperature differences are directly proportional to the energy using balances on

components. All thermocouples are shielded

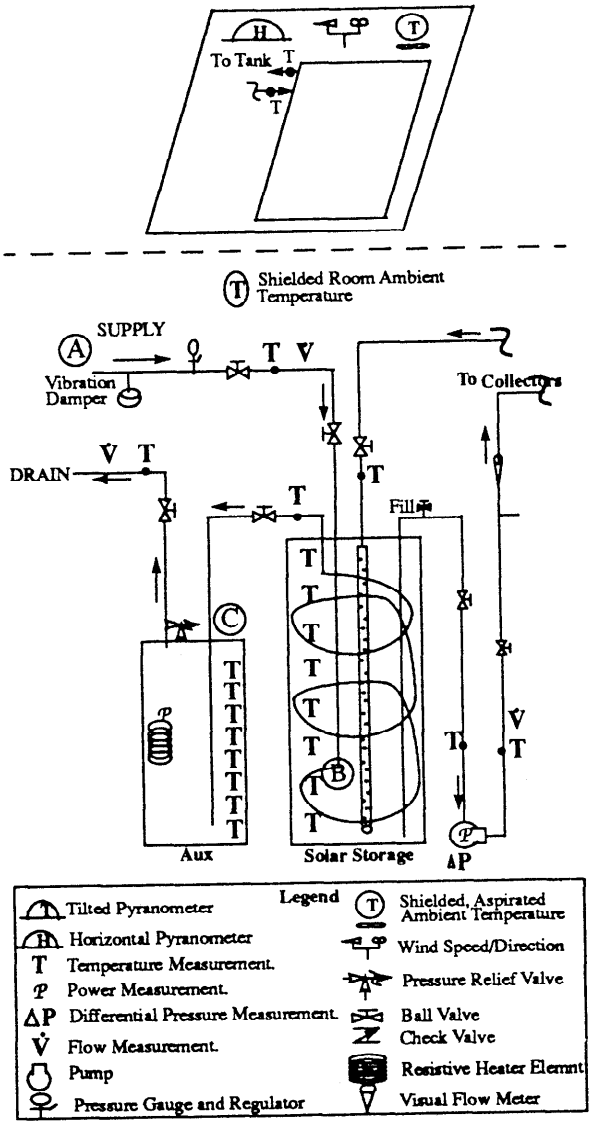

Fig 1. Weather station and system instrumentation

electrical conduit, and electrically isolated from the shields to prevent ground loops. Thermocouple arrays have been designed to measure tank temperatures at eight heights, where the spacing between thermocouples in the tank is uniform at one-eighth of the height of the tank. The return flow from the drainback collector enters a custom 0.35 m^3 (91gal) unpressurized solar storage tank. The pump circulates the solar storage tank water to the collectors and back to the solar storage tank at a flow rate of 3.9 x 10^{-5} m^3/s (0.6 gpm). The pump motor is rated at 29.8 W (1/25 hp). Fluid pumping of the system is accomplished using a bang-bang controller, with operation controlled by the temperature difference between the collector outlet and a point on the wall of the solar storage tank.

The load-side heat exchanger coil is 36.58 m (120 ft) of 0.0191 m (3/4 in) copper tubing coiled through the entire height of the solar storage tank. The coil is situated near the outer edge of the inside of the tank. The draw flow rate is 1.96 x $10^4 m^3/s$ (3.1 gpm). During a draw potable water from main supply flows to the bottom of the solar storage tank through a dep-tube, then spirals upward through the heat exchanger coil. The water then flows into the bottom of a standard 0.14 m3 (36 gal) auxiliary storage tank. Energy is transferred between the tanks only when there is a hot water draw.

3. EXPERIMENTAL RESULTS

Due to space limitations, only two days of the five days of test data will be presented. The two days are July 26 and July 27, 1994. These days were chosen as representative of the entire data set. July 26 was a fairly cloudy day and July 27 was a clear day with the highest solar insolation. As an indirect example of the heat exchanger performance, the solar storage tank temperatures are shown versus time in Figure 2. The top node of the tank is denoted by N=1, while the bottom node of the tank is denoted by N=8. The times when draws are done are denoted on the figures with a "D."

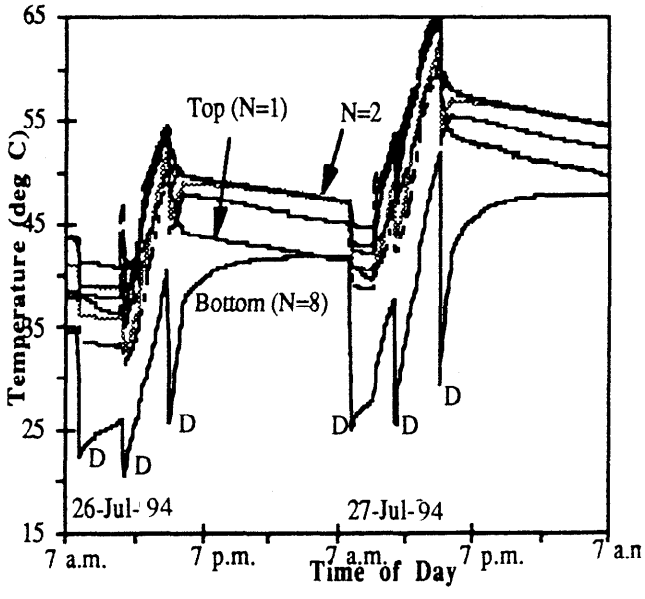

Fig. 2 Main solar storage tank temperatures

An average stratification of 10-15 _C is observed in the tank, with greater stratification in the afternoon, due to

the solar contribution. The very top node of the tank is cooler than several of the nodes below it. This is due mostly to an air gap which exists at the top of the tank when the collector is being pumped, and in part to the heat loss out the top of the tank. The stratification during a draw becomes more pronounced because the temperature in the bottom of the tank decreases by as much as 15°C while the temperature in the top of the tank decreases by only 3-5°C. This suggests that the mains supply water gains most of its energy from the bottom of the tank. During the day, between draws, the tank water temperature increases due to the solar contribution. This is especially noticeable in the bottom of the tank. During the night, the bottom of the tank actually warms up due to the conductive heat transfer from the rest of the tank.

Figure 3 shows the time histories of the temperature rise across the heat exchanger. The water mains supply temperature remains fairly constant at 16°C. As seen from Figure 3, initially the energy from the heat exchanger is very high, due to the four hours between draws, which has allowed the fluid in the heat exchanger to come into equilibrium with the tank water temperature. The residence time of water in the coil is 53 seconds at a draw flow rate of 1.96 x 10-4 m3/s (3.1 gpm). Thus, it is after about 1 minute that the heat exchange should begin to be well represented by traditional correlations.

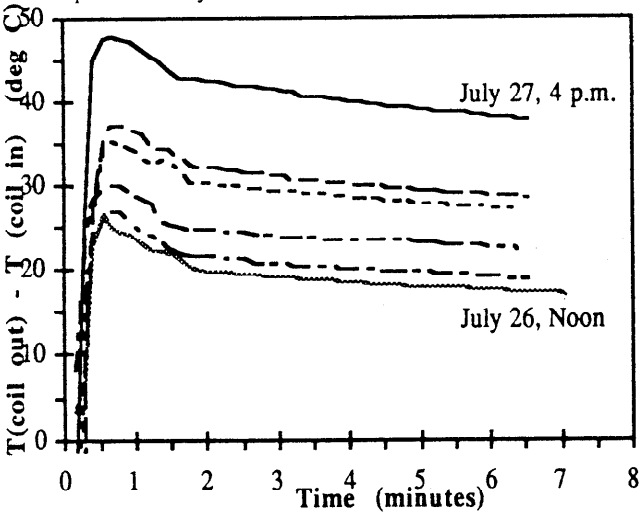

Fig. 3 Heat exchanger inlet and outlet versus time

4. ANALYSIS

4.1 Overall Heat Transfer Coefficient

The overall heat transfer resistance of the heat exchanger is comprised of three terms. The first is the inside convective coefficient due to forced flow through the coil (draw flow), the second is the conductance through the copper tubing, and the last is the outside convective heat transfer coefficient due to the natural convection flow around the coil.

The inside convective coefficient is determined using the Dittus and Boelter equation [Welty,1976] for the fluid being heated as the Reynold's number is 33,961 (the flow is turbulent), yielding a Nusselt number of 140.

$$(1)\quad Nu_i = \frac{h_i D}{k} = 0.023 Re_D^{0.8} Pr^{0.4}$$

The corresponding convective coefficient is 4,890 $W/m^2°C$ (861 $Btu/hrft^2°F$). The conductance through the copper tubing is negligible.

The outside convective coefficient is predicted using four methods. The representative temperature difference used for each method is 12°C. This is based on the 10-15°C difference between the tank temperature and the supply temperature during a draw. The results of these methods are summarized in Table 1. Method (a) uses a correlation for a vertical cylinder, given as equation (2) from Kakac [1987], which is valid for all Ra_D. The Ra number was calculated using the large coil diameter (0.66 m, 26") as a characteristic length. This correlation actually was developed for an isothermal solid wall in an infinite fluid, with no influence from the surrounding wall.

$$(2)\quad Nu_o = \frac{4}{3}\left[\frac{7GrPr^2}{5(20+21Pr)}\right]^{\frac{1}{4}} + \frac{4(272+315Pr)L}{35(64+63Pr)D}$$

Method (b) assumes that the coil area is a vertical flat plate. This could be inferred since $D/L > 35/GrD^{1/4}$ [Kakac, 1987], with less than 5% error. The correlation, given as equation (3), is based on the height of the tank, L (1.4 m, 55").

$$(3)\quad Nu_o = \left\{0.825 + \frac{0.387Ra^{1/6}}{\left[1+(0.492/Pr)^{9/16}\right]^{8/27}}\right\}^2$$

Method (c) is for flow over a horizontal cylinder. The Ra number is based on the diameter of the tubing (0.019 m, 0.75"). The McAdams correlation [Welty, et. al., 1976], which holds for $10^4 < Ra_D < 10^9$, is:

$$(4)\quad Nu_o = 0.53(Gr_D Pr)^{1/4}$$

Method (d) uses the correlation equations (5) and (6), from Farrington and Bingham [1987]. Note that they recommend using the LMTD as the driving potential.

Further, they recommend C=0.9 and m=1/4 (for laminar flow).

(5) $Nu_o = CR_D^m$

(6) $$LMTD = \frac{(T_{Bot} - T_{HX,in}) - (T_{TopMax} - T_{HX,out})}{\ln\left(\frac{T_{TnkBot} - T_{HX,in}}{T_{TnkMax} - T_{HX,out}}\right)}$$

Finally, the test results were reduced as shown in equation (7). In all cases, the area, A, is equal to 1.86 m^2 (20 ft^2).

(7) $$h_{meas} = \frac{\dot{Q}_{drw}}{A(T_{tnk} - T_{coil})} = \frac{(\dot{m}c_p)_{drw}(T_{HX,out} - T_{HX,in})}{A(T_{tnk} - T_{coil})}$$

The results of the calculations are provided in Table 1. Note that method (c) agrees with the measured value to within 20%. The coils within the tank are stacked on top of one another with almost no gap in between each successive coil, which seem to enhance the heat transfer over a single horizontal cylinder. This is attributed to the vortex shedding off of each coil. Therefore, the flow is turbulent over each coil, which increases the heat transfer.

TABLE 1. HEAT TRANSFER PROPERTIES

Method	Eqn	Ra	h_o (W/m^2C)	UA (W/C)	Q (W)
(a)	(2)	6.5×10^{11}	337	450	6,750
(b)	(3)	1.6×10^{12}	719	905	37,575
(c)	(4)	6.8×10^{9}	834	1,321	19,815
(d)	(5)	4×10^{5}	791	1,266	12,660
meas.	-	5×10^{6}	1,040	1,600	24,000

Also, note the poor agreement (47%) from method (d). This is perhaps due to the short duration of our draws (7 minutes) relative to the long duration of Farrington and Bingham's tests (3 to 4 hours). Only a small fraction of energy is extracted from the tank over 7 minutes, a "shallow" draw, while in contrast the tank is nearly completely purged of energy over 4 hours, a "deep" draw. This makes the LMTD a poor predictor of performance for situations where the tank temperature changes little. A load-side heat exchanger of this design appears to be relatively ineffective at extracting energy from the tank over "shallow" draw profiles. Therefore, it probably leads to substantially sub-optimal performance of the system.

4.2 Effectiveness

The heat exchanger effectiveness was calculated using equation (8).

(8) $$\varepsilon = \frac{\Delta Q}{\Delta Q_{max}} = \frac{m_{drw}C_p(T_{HX,out} - T_{HX,in})}{m_{drw}C_p(T_{TnkMax} - T_{HX,in})}$$

Figure 4 presents the calculated effectiveness for over two days of draw data. The average calculated effectiveness is 0.78 for all data. The first minute of data is the purging of the warmed coil water. The energy contained in the "hump," over and above the 0.78 average effectiveness, is only 3% of the total draw energy. The spread in the curves is due to the dependence of the outside convective heat transfer coefficient on the temperature difference. Notice in Figure 2 that the tank temperature had not risen significantly between the 8 a.m. draw and the noon draw on July 26, 1994. This was a cloudy day and the pump had not operated much; hence the temperature difference is lower, as is the effectiveness. Also, it was found that the effectiveness is not affected by whether or not the pump is on or off during the actual draw.

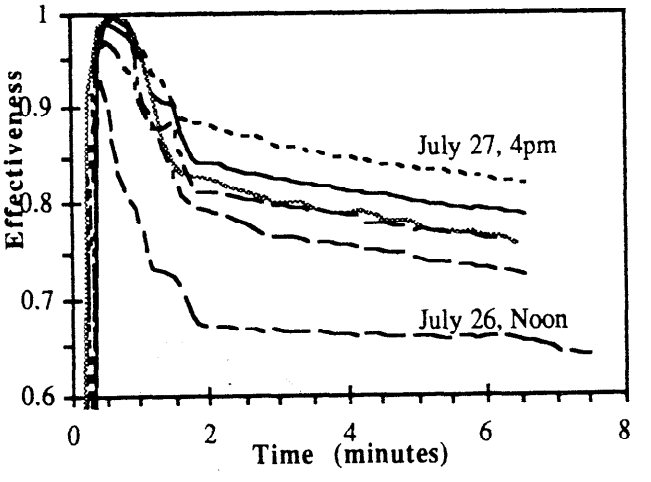

Fig. 4 Heat exchanger effectiveness

In trying to correlate heat exchanger effectiveness with our experimental data, it is noted that equation (9) for a counterflow heat exchanger results in a calculated effectiveness of 0.74. The equation is from Kays and London [1964].

(9) $$\varepsilon = \frac{N_{TU}}{1 + N_{TU}}, N_{TU} = \frac{UA}{C_{min}}$$

5. SIMULATION RESULTS

It is also important to assess the performance of the solar system vis a vis the SRCC efforts, which seek to rate system performance using TRNSYS [Klein et al., 1994] simulations [Burch et al., 1993]. One of the overall goals is to match the model to experimental data by adjusting the model parameters to represent more accurately the physical properties of the system.

A TRNSYS module for modeling a load-side heat exchanger did not exist in version 13.1 at the time of this work, so the tank models were "tricked" into simulating one by including a heat exchanger effectiveness parameter. The measured average heat exchanger effectiveness of 0.78 was used to adjust the load flow out of the solar storage tank. The replacement fluid into the solar storage tank, since the flow into the main solar storage tank from the "hot source" (collectors) is not equal to the solar storage tank load flow, is at mains supply temperature. The flow from the "hot source" (the solar storage tank) into the auxiliary storage tank is zero. The temperature entering the auxiliary storage tank as replacement fluid is also adjusted by the effectiveness. The draw flow off of the auxiliary tank is the experimental value.

The results are shown in Table 2, indicating excellent agreement.

TABLE 2. MEASURED AND TRNSYS RESULTS

Quantity	Measured$_1$	TRNSYS	%Error
Q_{usefu} (MJ)	186	184	1.1
Q_{draw} (MJ)	114	115	-0.9

6. CONCLUSIONS

The external flow around the coil is laminar, natural convection, while the inside is turbulent, forced convection. The inside heat transfer coefficient contributes little to the overall thermal resistance, while the outside resistance is dominant. The best agreement for the outside heat transfer coefficient is obtained using the correlation for free convection from a horizontal cylinder, with a 20% enhancement most probably due to an increase in the heat transport attributed to turbulence generated from flow over each coil in the heat exchanger. An average effectiveness of 78% was calculated from experimental data. When used in a TRNSYS model, agreement to within 1% of energy delivered was achieved, indicating that for "shallow" energy draws, a constant effectiveness model yields excellent agreement with observations.

7. REFERENCES

(1) ASHRAE, "Standard 95-85: Method of Testing to Determine the Thermal Performance of Solar Domestic Hot Water Systems," ASHRAE, Atlanta, GA, 1985
(2) Farrington, R. B., and Bingham, C. E., "Testing and Analysis of Load-Side Immersed Heat Exchangers for Solar Domestic Hot Water Systems," Prepared for the U.S. Department of Energy, Contract No. DE-AC02-83CH10093, Solar Energy Research Institute, Golden, CO, 1987
(3) Kakac, Sadik, et. al., Handbook of Single-Phase Convective Heat Transfer, Ch. 12 & 13, John Wiley and Sons, New York, NY, 1987
(4) Kays, W. M., and London, A. L., Compact Heat Exchangers, Second Edition, McGraw-Hill Book Co., New York, NY, 1964
(5) Klein et al., "TRNSYS - A Transient System Simulation Tool, Ver. 14.1," Solar Energy Laboratory, University of Wisconsin, Madison, WI, 1994
(6) SRCC, January, "Standard OG-300: Directory of Solar Water Heating Systems Meeting Minimum Operating and Performance Requirements," Publication of the Solar Rating and Certification Corporation, Washington, D.C., 1993
(7) Welty, J. R., et. al., Fundamentals of Momentum, Heat and Mass Transfer, Second Edition, John Wiley & Sons, Inc., New York, NY, 1976